◆ Human Brain Mapping 6:301–315(1998) ◆

# Intersubject Variability of Functional Areas in the Human Visual Cortex

**Mohammed K. Hasnain,[1,2] Peter T. Fox,[1–5]* and Marty G. Woldorff[1,3]**

[1]*Research Imaging Center, University of Texas Health Science Center at San Antonio, San Antonio, Texas*
[2]*Department of Physiology, University of Texas Health Science Center at San Antonio, San Antonio, Texas*
[3]*Department of Radiology, University of Texas Health Science Center at San Antonio, San Antonio, Texas*
[4]*Department of Medicine (Neurology), University of Texas Health Science Center at San Antonio, San Antonio, Texas*
[5]*Department of Psychiatry, University of Texas Health Science Center at San Antonio, San Antonio, Texas*

**Abstract:** Intersubject variability of striate and extrastriate areas was mapped by conjoined use of positron emission tomography (PET) and magnetic resonance imaging (MRI). We used two dynamic bowtie-shaped random-dot patterns centered symmetrically around the vertical- and horizontal-meridian, respectively, presented during sequential PET scans in 11 subjects. Control condition was simple fixation on a central dot in absence of a surrounding random dot pattern. V1, V2, VP, V3, V3a, V4, V5, and "wordform" areas were identified. After spatial normalization to Talairach atlas space, mean locations and standard deviations about these mean locations for x-, y-, and z-axes were calculated for each area in both hemispheres and compared for differences. The mean standard deviation for all axes across all areas tested was found to be small (4.9 mm). No significant differences were found in the mean standard deviations for the x-, y-, and z-axes in the left hemisphere vs. their counterparts in the right hemisphere. However, when mean standard deviations in both hemispheres were polled together by axis, the mean standard deviation for the y-axis (5.3 mm) was found to be significantly different from the mean standard deviation for the x-axis (4.3 mm). Furthermore, in the left hemisphere, the mean standard deviation for the z-axis (5.7 mm) was significantly greater than the mean standard deviation for the x-axis (3.9 mm). The values reported in this study for mean location and standard deviation of visual areas can be used to establish confidence intervals for distinguishing normal variations from pathology and consequent brain reorganization. *Hum. Brain Mapping 6:301–315, 1998.* 

**Key words:** positron emission tomography; retinotopy; brain mapping; striate cortex (V1); extrastriate cortex; V2; VP; V3; V3a; V4; V5

## INTRODUCTION

Despite the quickened pace with which we are learning about the visual cortex in man, little has been done to quantify intersubject variability in the location of the multiple visual areas identified. A study of variability in the functional map of the cerebral cortex is important both practically and theoretically. Knowledge of the frequency, magnitude, types, and source of normal variations is vital not only for physiologic studies but also for pathological assessment. Lacking a

Contract grant sponsor: Research Imaging Center, University of Texas Health Science Center at San Antonio, San Antonio, Texas; Contract grant sponsor: Human Brain Project; Contract grant number: P20 MH / DA52176.

Performed at the Research Imaging Center, University of Texas Health Science Center at San Antonio, San Antonio, Texas.

*Correspondence to: Peter T. Fox, M.D., Director, Research Imaging Center, University of Texas Health Science Center at San Antonio, 7703 Floyd Curl Drive, San Antonio, TX 78284–6240. Phone: (210) 567–8150; Fax: (210) 567–8152

Received for publication 19 June 1997; accepted 26 March 1998

comprehensive knowledge of normal variability, disease-induced variations cannot be detected with confidence. Moreover, insight into the phylogenetic and ontogenetic forces that govern the development of the functional areas of the cerebral cortex must be predicated on a knowledge of its variations. Since an increasing number of studies are now reporting results in stereotaxic coordinate space, it is important to know the residual variance that is left after normalization into such a space.

Recently, echoplanar functional magnetic resonance imaging (fMRI) studies by Sereno et al. [1995] and DeYoe et al. [1996] have demonstrated the feasibility of identifying early extrastriate areas in the occipital lobe using retinotopic phase-encoded stimuli. These studies were based on literature describing the retinotopic organization of early extrastriate areas in nonhuman primates [Daniel and Whitteridge, 1961; Zeki, 1969; Zeki and Sandeman, 1976; Van Essen and Zeki, 1978; Newsome et al., 1986; Gattas et al., 1988] and also on lesion analysis data describing visual field defects in man [Holmes, 1945; Clarke and Miklossy, 1990; Horton and Hoyt, 1991]. The nomenclature for visual areas (V1, V2v, V2d, VP, V3, V3a, V4, and V5(MT)) was adapted for man from that described by Felleman and Van Essen [1991] for the macaque monkey. Both imaging and the lesion-analysis studies indicate that a retinotopic organization similar to that in the macaque exists in man such that the calcarine sulcus represents the contralateral horizontal-meridian in V1, whereas the dorsal V1/V2d border represents the inferior vertical-meridian and the ventral V1/V2v border represents the superior vertical-meridian. Thereafter, the borders of visual areas V2d/V3 and V2v/VP represent the contralateral horizontal-meridian. Another vertical-meridian representation occurs at the anterior VP border and at the V3/V3a border. Thus, alternating vertical- and horizontal-meridian representations occur at the borders of early visual areas V1/V2d, V2d/V3, and V3/V3a dorsal to the calcarine sulcus, and at V1/V2v, V2v/VP, and VP/V4 borders ventral to the calcarine sulcus. However, none of these studies provide a quantitative analysis of the intersubject variability in location of the multiple areas in the extrastriate cortex of man. In the present investigation we assessed the spatial variability in Talairach space of early extrastriate areas, as identified using positron emission tomography (PET), thus reporting results in an objective and generalizable framework for a normal population.

## METHODS

### Tomographic and tracer techniques

PET data were acquired as regional distributions of tracer-associated radiation. Water labeled with oxygen-15 ($H_2{}^{15}O$, half-life 123 sec) was used as a freely diffusible blood-flow tracer to measure increases in regional cerebral blood flow (rCBF) caused by increased neuronal activity in response to the stimuli [Raichle et al., 1983; Herscovitch et al., 1983; Raichle, 1987]. Fifteen parallel slices of blood flow images were acquired with a GE/Scanditronix 4096 PET camera with a center-to-center interslice distance of 6.5 mm. Images were reconstructed at a resolution of 6 mm full width at half maximum (FWHM) for simultaneously occurring events. Sequential events, however, could be distinguished from one another at a much higher resolution [Fox et al., 1986]. This phenomenon, also called Vernier acuity, is well-known in signal detection theory [Lahti, 1965].

Each scan started with the stimulus presentation. This was followed by an intravenous bolus of $^{15}O$-labeled water (half-life 123 sec) administered as 8–10 ml of saline containing 60–70 mCi. As the tracer entered the field of view (the brain), the rapid rise in the coincidence counting rate triggered a 90-sec scan. The stimulus presentation ended 40 sec after the start of the scan. A further 50 sec of data were acquired, since PET data are a cumulative record of the tracer-associated radiation distribution that persists after the end of the stimulus presentation for up to 1 min. An 11-min interscan interval was employed for reestablishing resting-state levels of rCBF and for isotope decay ($>$5 half-lives). Each of the subjects also underwent an anatomic MRI scan of the brain in an Elscint Prestige2-tesla machine at a spatial resolution of $1 \times 1 \times 1.5$ mm.

### Subject population and preparation

Eleven normal right-handed male volunteers between age 18–35 years were recruited. Handedness restriction was assessed by history and was used to avoid confounds due to differences in hemispheric anatomy between left- and right-handed people. Informed consent was obtained as prescribed by the institutional review board of the University of Texas Health Science Center at San Antonio. A medical history battery questioned the subjects about neurological, cardiovascular, and psychiatric history.

During scanning, the subjects were placed supine with the head resting on a foam-padded head holder.

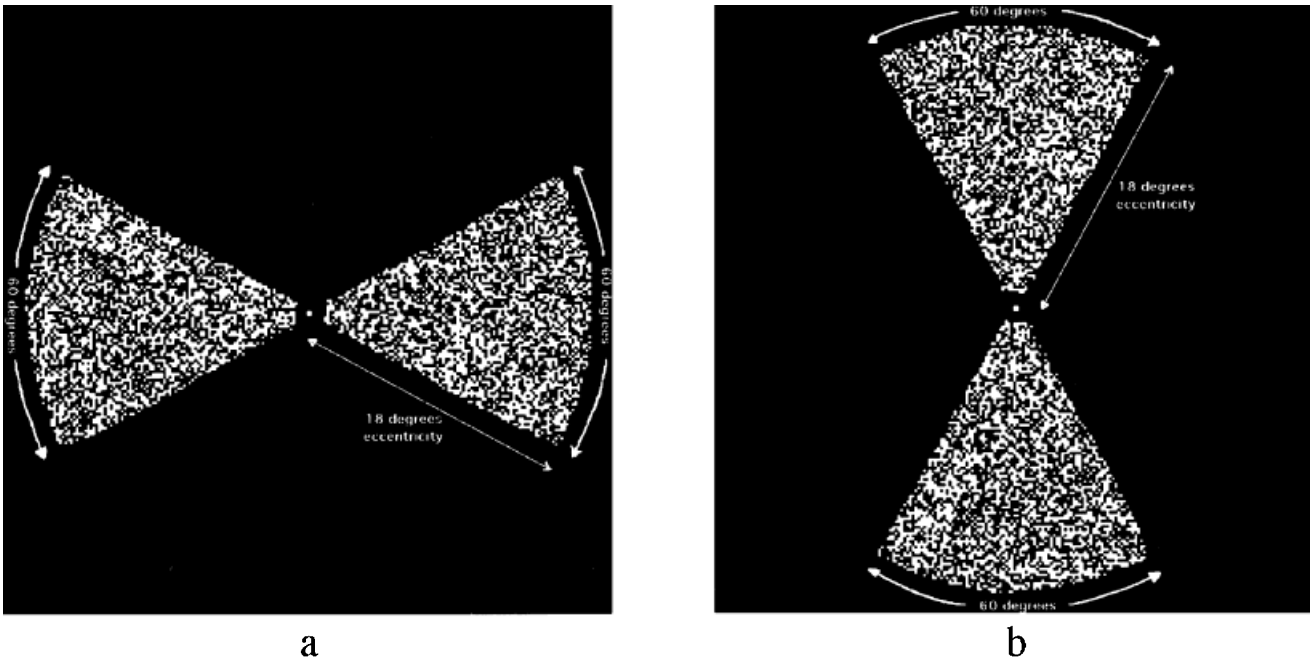


**Figure 1.**
**a:** Horizontally oriented random-dots stimulus. **b:** Vertically oriented random-dots stimulus. Both stimuli were random-dot patterns with 50% density on a dark background, changing at 8 Hz to maximize response intensity [Fox and Raichle, 1985]. Stimuli extended radially to 18° eccentricity and were 60° in width.

The angle of the sections was selected such that it was as perpendicular to the calcarine sulcus as possible. The head position was adjusted, aided by laser alignment beams and ear-canal fiducials, until the head lay symmetrically about the midsagittal plane. A tightly fitted, thermally molded, plastic facial mask was used to immobilize the head. The position of the first slice was marked on the mask for reference.

### Stimuli and task

Subjects were scanned under three experimental conditions. Task 1 involved passive fixation on a central dot surrounded by a horizontally oriented random-dot pattern changing at 8 Hz [Fox and Raichle, 1985] and extending to 18° eccentricity (HRD, Fig. 1a). Task 2 involved passive fixation on a central dot surrounded by a vertically oriented random-dot pattern changing at 8 Hz and extending to 18° eccentricity (VRD, Fig. 1b). The random-dot patterns appeared only in two 60° arcs centered around the horizontal- and vertical-meridian, respectively. The foveal region, except for the fixation point, was left out of the stimuli such that no pattern of random dots appeared within 1° eccentricity of the fixation point. Control involved fixation on a central dot in absence of any surrounding pattern (FIX). Multiple independent trials of each condition greatly enhance the signal-to-noise ratio and are essential for individual subject analysis. Therefore, to assure optimal data quality, each of the three experimental conditions was repeated three times in the sequence: FIX-HRD-VRD-FIX-VRD-HRD-FIX-HRD-VRD. This design controls for order effects and allows collection of sufficient and equivalent scanning data for each condition. However, one of the subjects underwent only eight scans in the sequence HRD-VRD-FIX-VRD-HRD-FIX-HRD-VRD, due to cumulative dose constraints.

### Image analysis

#### *Physiological and anatomical normalization*

The PET images were masked using 30% of the maximum value threshold to the brain surface. Interscan movement correction was performed using the algorithm of Woods et al. [1993]. The sinuses were manually masked out. Blood-flow-related activity in

each voxel was divided by the mean whole-brain activity to yield a ratio that is independent of variations unrelated to the stimulus condition [Fox et al., 1985]. The PET images for each individual were anatomically normalized into the proportional, bicommissural coordinate space of Talairach and Tournoux [1988], using an affine, nine-parameter algorithm [Lancaster et al., 1995]. The MRI images from each individual were also anatomically normalized into the same space, and the PET images were coregistered to the corresponding individual's normalized MRI images within one voxel (2 mm error) for each axis (x, y, and z).

### *Statistical methods*

Images acquired during the control state were subtracted from images acquired during the HRD and VRD stimuli conditions, respectively, to create subtraction images representing task-associated changes in rCBF. Pixels that were not common to both images in a subtraction pair were discarded. This resulted in three subtraction images for the HRD condition and three for the VRD condition. The three subtraction images within each condition were averaged together. Statistical analysis of the averaged subtraction images was based on the signal-to-noise ratio of the focal responses relative to the residuals in the inactivated brain. Because of the functional specificity of the brain, relatively few regions are perturbed by an intervention. Unchanged areas appear as random noise background against which regional changes form local maxima and minima. Three-dimensional (3-D) interpolation converted the tomographic data set into a 3-D matrix, to prepare for local maximum search. This search identifies all discrete regional changes, both positive and negative, within the image of rCBF. A search kernel of $3 \times 3 \times 3$ voxels (voxel size 2 mm) was employed. The magnitudes and 3-D locations of the local maxima were reported as regions of interest, placed at the center of mass of regional change. The output of the local maximum search is the change distribution across the brain volume. Change distribution analysis (CDA) identifies physiological responses as outliers in the noise distribution by using a one-sided gamma-2, a modification of the conventional outlier detection statistic [Fox et al., 1988]. Extrema with z-scores $>1.96$ were considered significant.

The Lillifors test, a variant of the Kolmogrov-Smirnov goodness of fit test, was employed for statistical testing of departures from normality of the spatial distribution in the x-, y-, and z-axes. This test is applicable for sample sizes ranging from 5–10,000. Confidence intervals for standard deviations, homogeneity of a group of variances, and statistical difference between pairs of variances were determined by standard biostatistical analyses [Zar, 1984].

### *Functional labeling of local maxima*

Activation studies by Sereno et al. [1995] and DeYoe et al. [1996], as well as lesion studies by Holmes [1945] and Horton and Hoyt [1991], have established the calcarine sulcus as the site of the horizontal-meridian representation in the primary visual cortex (V1) of man. Based on this literature, the horizontal-meridian activation in V1 was identified using calcarine anatomy as the reference. The data set was viewed using a 3-D visualization tool [Lancaster et al., 1995]. All extrema that formed a contiguous cluster of activation (z-score $>2$) and were within 6 mm of the calcarine were included as part of the V1 horizontal-meridian representation. If no such extrema were found (which occurred in 2 out of 22 hemispheres), an extremum that was closest to the calcarine and had a z-score of $>2.5$ was considered to be part of the V1 horizontal-meridian representation. Following the cortical surface ventral to the calcarine, the next horizontal-meridian activation site was identified, and all extrema within this activated area were considered to be part of the V2v/VP border. Similarly, following the cortical surface dorsal to the calcarine, a horizontal-meridian activation site immediately dorsal to the V1 horizontal-meridian representation was identified and all extrema contributing to this activation site were considered to be part of the V2d/V3 border. The three sets of extrema representing the horizontal-meridian activations in V1, at V2v/VP, and at V2d/V3 borders were mutually exclusive (Fig. 2a). Vertical-meridian representations were analyzed such that the vertical-meridian activation immediately ventral to the V1 horizontal-meridian activation site was identified as the V1/V2v border. Vertical-meridian representation immediately ventral to the V1/V2v border was identified as representing the anterior border of area VP. Similarly, the vertical-meridian activation immediately dorsal to the V1 horizontal-meridian representation was identified as the V1/V2d border, and the vertical-meridian activation dorsal to the V1/V2d border was identified as the V3/V3a border (Fig. 2b). Extrema coordinates within each region of activation were averaged together to yield the coordinates for the center of activation of that

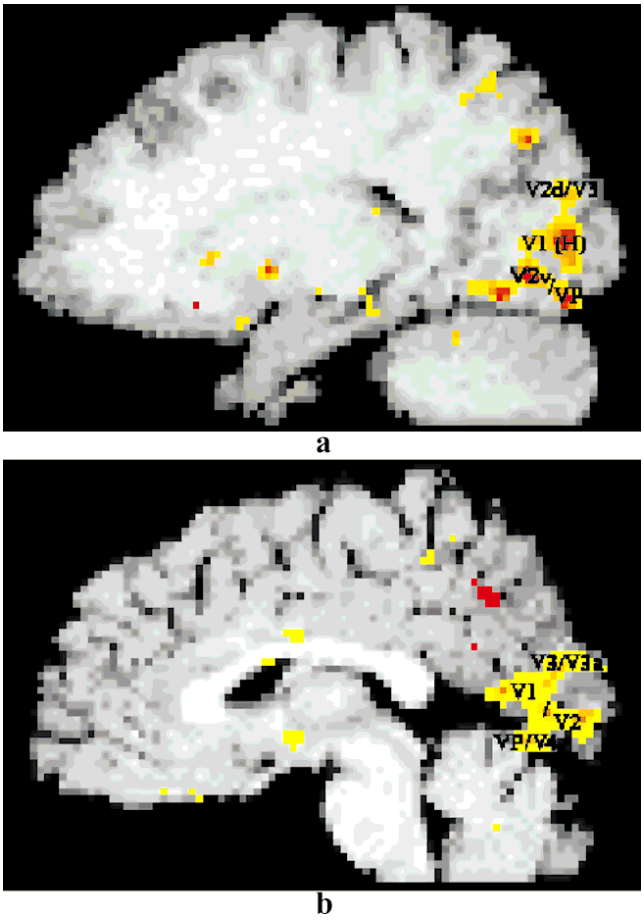


**Figure 2.**
**a:** Image of change in blood flow 18 mm to the right of the midsagittal line in an individual induced by horizontally oriented random-dot patterns, thresholded to z = 2.33 ($P < 0.01$) and overlaid onto corresponding MRI. **b:** Image of change in blood flow 4 mm to the right of the midsagittal line in the same individual, induced by vertically oriented random-dot patterns, thresholded to z = 2.33 ($P < 0.01$) and overlaid onto corresponding MRI.

region. The coordinates for the center of a particular visual area were obtained by averaging the coordinates for its borders, e.g., the center of V2v was obtained by averaging the coordinates for its borders V1/V2v and V2v/VP. For areas V4 and V5 a directed local-maximum search strategy was performed as follows. A pair of horizontal- and vertical-meridian activation sites (separated by <10 mm and each with a z-score of >2 ($P < .025$)), lying closest to the previously reported mean coordinates for area V4 by Zeki et al. [1991], were identified. Another pair of horizontal- and vertical-meridian activation sites (separated by <10 mm and each with a z-score of >2 ($P < .025$)), were identified that lay closest to the previously reported mean coordinates for area V5 by Watson et al. [1993]. Responses identified as V1, V2v, V2d, V3, and V3a were excluded from this directed local-maximum search except for the anterior VP border, which may also be part of the area V4. If no paired responses meeting the above criteria were found within a fixed radius of 2 cm of the previously reported mean coordinates for an area, the response for that area in that individual was considered to be absent. This approach, first implemented by Fox and Pardo [1991], has been shown to resolve group activations that are not closely clustered, and a comparable approach was also used by Hunton et al. [1996] in their analysis of functional-anatomical variability in neuroimaging studies.

A similar search was performed in the inferior occipital lobe for the "wordform" area as defined by Petersen et al. [1990]. This area is best known for activating in response to orthographic stimuli [Posner and Raichle, 1994]. However, it is also known to activate in response to nonword-like stimuli [Parsons et al., 1995] and may have a specific role in assembling visual percepts and images as a part of the left lateralized object recognition system [Farah, 1991]. Responses identified as other visual areas were excluded from the search for the "wordform" area as well.

## RESULTS

### Frequency of observation

Regions of activation alternating between those due to the HRD stimulus and those due to the VRD stimulus were observed extending outwards from the V1 horizontal-meridian representation (Fig. 3). This pattern of activation continued up to area V3a on the dorsal occipital surface and down to the anterior border of area VP on the ventral occipital surface. All of these areas were consistently activated and reliably localized. The frequency with which focal responses could be identified for a given area ranged between 70–100% across subjects (Table I). Areas V1, V2, VP, and V4 were identified in both hemispheres of all 11 individuals. Areas V2d, V3, and V3a were detectable in the right hemispheres of all individuals. In the left hemisphere these areas were resolvable in 10 out of 11 individuals. In the left hemisphere of the remaining individual, the V2/V3 border representing the horizon-

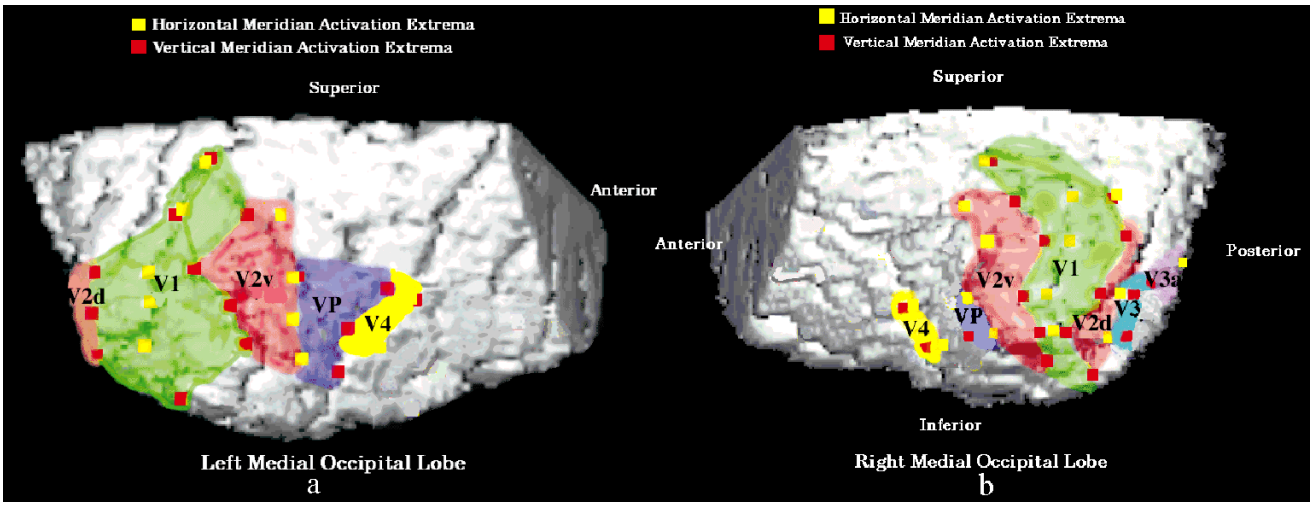


**Figure 3.**

**a:** Medial view of the left occipital lobe of an individual with maxima (extrema) of cerebral blood flow change induced by the stimuli superimposed. **b:** Medial view of the right occipital lobe of an individual with maxima (extrema) of cerebral blood flow change induced by the stimuli superimposed. Calcarine sulcus represents the contralateral horizontal-meridian in V1, whereas the dorsal V1/V2d border represents the inferior vertical-meridian and the ventral V1/V2v border represents the superior vertical-meridian. Thereafter, the borders of visual areas V2d/V3 and V2v/VP represent the contralateral horizontal-meridian. Another vertical-meridian representation occurs at the anterior VP border and at the V3/V3a border. Color-shaded regions are putative visual areas deduced from the retinotopic organization of early visual areas boundaries, alternating between horizontal- and vertical-meridian representations.

tal-meridian was not separable from the horizontal-meridian representation in V1. This led to a failure to identify the borders of areas V2d, V3, and V3a in the left hemisphere of this individual. Area V4 was found in all 22 hemispheres examined. The mean distance between the identified left V4 and the corresponding coordinates of Zeki et al. [1991] was 5.2 mm, and the mean distance between the identified right V4 and the corresponding coordinates of Zeki et al. [1991] was 10.4 mm (Table II). V4 was usually found to be adjacent to area VP but not always. The search for the vertical- and horizontal-meridian activations around the "word-form" area led to identification in 10 out of 11 subjects. The mean distance between the identified "wordform" and the corresponding coordinates of Petersen et al. [1990] was 6.9 mm. Least readily discernible, however, was area V5. Nine out of 11 subjects showed a response to both the horizontal- and vertical-meridian stimuli in the right hemisphere. The mean distance between the coordinates for right V5 and the corresponding coordinates of Watson et al. [1993] was 3.8 mm. In the left hemisphere, 8 out of 11 subjects showed a response to both horizontal- and vertical-meridian stimulation, with the mean coordinates being within 5.4 mm of those reported by Watson et al. [1993] for left V5. The reason for the low frequency of detection for V5 may be due to the nature of the stimulus (optimal stimulus for V5 is coherently moving objects, whereas randomly changing dots were employed in this study). Activations were also seen in the temporal and parietal lobes (see Fig. 2).

## Response magnitude

Response magnitude was calculated as percentage blood-flow change (%BF) above baseline, and significance of response was calculated as z-scores (Table I). The average response magnitude of all 24 regions sampled in 11 subjects was 25.9%, with a standard deviation of 9.3%. The mean response for horizontal-meridian stimulation was 25.6% with a standard deviation of 10.1%, and for vertical-meridian it was 26.2% with a standard deviation of 8.6%. The difference between the mean response magnitude for horizontal- vs. vertical-meridian stimulation was nonsignificant. The two greatest mean responses were 36.4% and 33.2% above baseline condition at the left V1/V2 border and at the right V1 horizontal-meridian representation, respectively. The two smallest %BF changes

**TABLE I. Response magnitude and frequency of detection***

| Area | Frequency of detection (%) | Mean response magnitude of maximally activated voxels in %BFΔ above base line (SD) | Mean response significance of maximally activated voxels Z-score |
|---|---|---|---|
| Left hemisphere (N = 11) | | | |
| V1 (H) | 100 | 30.7 (6.64) | 4.24 ($P < 0.0001$) |
| V1/V2v (V) | 100 | 23.6 (7.51) | 3.38 ($P < 0.0004$) |
| V1/V2d (V) | 100 | 36.4 (14.4) | 4.1 ($P < 0.0001$) |
| V2v/VP (H) | 100 | 30.3 (13.23) | 3.52 ($P < 0.0002$) |
| V2d/V3 (H) | 91 | 26.6 (10.03) | 3.15 ($P < 0.0008$) |
| Anterior VP (V) | 100 | 23.4 (7.27) | 3.19 ($P < 0.0007$) |
| V3/V3a (V) | 91 | 24.8 (6.68) | 3.0 ($P < 0.0013$) |
| V4 (H) | 100 | 27.4 (12.16) | 3.39 ($P < 0.0003$) |
| V4 (V) | 100 | 23.0 (3.09) | 3.01 ($P < 0.0013$) |
| V5 (H) | 73 | 22.7 (11.22) | 2.54 ($P < 0.0055$) |
| V5 (V) | 73 | 26.2 (9.11) | 2.83 ($P < 0.0023$) |
| "Wordform" (H) | 91 | 32.2 (12.58) | 2.99 ($P < 0.0014$) |
| "Wordform" (V) | 91 | 31.1 (9.31) | 2.92 ($P < 0.0018$) |
| Right hemisphere (N = 11) | | | |
| V1 (H) | 100 | 33.2 (13.8) | 4.33 ($P < 0.0001$) |
| V1/V2v (V) | 100 | 25.2 (5.8) | 3.74 ($P < 0.0001$) |
| V1/V2d (V) | 100 | 25.4 (7.6) | 3.58 ($P < 0.0002$) |
| V2v/VP (H) | 100 | 30.9 (7.3) | 3.93 ($P < 0.0001$) |
| V2d/V3 (H) | 100 | 26.1 (7.3) | 3.28 ($P < 0.0005$) |
| Anterior VP (V) | 100 | 24.0 (14.2) | 2.98 ($P < 0.0014$) |
| V3/V3a (V) | 100 | 26.4 (7.2) | 3.23 ($P < 0.0006$) |
| V4 (H) | 100 | 26.1 (7.5) | 3.39 ($P < 0.0003$) |
| V4 (V) | 100 | 26.1 (8.7) | 3.33 ($P < 0.0004$) |
| V5 (H) | 82 | 22.6 (10.3) | 2.88 ($P < 0.002$) |
| V5 (V) | 82 | 25.1 (7.5) | 2.71 ($P < 0.0034$) |

* H, responses to horizontally oriented stimulus; V, responses to vertically oriented stimulus; SD, standard deviation.

of 22.6% and 22.7% occurred at the horizontal-meridian representation of the right and the left V5, respectively. However, there was considerable variance within each data set. For example, the greatest %BF change of 62.7% occurred at the anterior border of the right VP of an individual. Although statistical significance (in terms of z-scores) did not always follow the same order as %BF change, the two were

**TABLE II. Comparison of V4, V5, and "wordform" area coordinates with previous studies**

| Area | Study | Talairach coordinates: Lx, Rx (mm) | Ly, Ry (mm) | Lz, Rz (mm) |
|---|---|---|---|---|
| V4 | Present study | −21.8, 19.8 | −65.6, −72.7 | −10, −12 |
| | Zeki et al. [1991] | −26, 20 | −68, −66 | −8, −4 |
| V5 | Present study | −39, 41.3 | −71.9, −64.8 | −0.8, 1.6 |
| | Watson et al. [1993] | −44, 40 | −70, −68 | 0, 0 |
| "Wordform" area | Present study | −19.8 | −70.8 | 1.9 |
| | Petersen et al. [1990] | −23 | −65 | 4 |

**TABLE III. Mean location and standard deviation of visual areas**

| Area | Mean location (mm) (Talairach coordinates) | | | Standard deviation (mm) | | | Frequency of detection (%) |
|---|---|---|---|---|---|---|---|
| | x | y | z | x | y | z | |
| Left hemisphere (N = 11) | | | | | | | |
| V1 | −7.2 | −82.5 | −1.9 | 3.3 | 5.3 | 7.5 | 100 |
| V2v | −7.7 | −75.3 | −7.5 | 4.2 | 5.1 | 4.9 | 100 |
| V2d | −11.7 | −91.5 | 2.7 | 4.6 | 4.3 | 8.6 | 91 |
| VP | −13.7 | −72.2 | −10.2 | 2.0 | 7.6 | 5.1 | 100 |
| V3 | −17.9 | −89.6 | 5.9 | 5.9 | 5.0 | 7.5 | 91 |
| V3a | −25.7 | −83.8 | 11.0 | 2.9 | 4.9 | 6.1 | 82 |
| V4 | −21.8 | −65.8 | −9.9 | 4.5 | 5.0 | 3.6 | 100 |
| V5 | −39.0 | −71.9 | −0.8 | 2.6 | 4.2 | 4.1 | 73 |
| ‘‘Wordform’’ | −19.8 | −70.8 | 1.9 | 4.6 | 3.7 | 3.8 | 91 |
| Mean standard deviation | | | | 3.9 | 5.0 | 5.7 | |
| Right hemisphere (N = 11) | | | | | | | |
| V1 | 6.2 | −79.9 | 0.9 | 2.6 | 5.7 | 5.0 | 100 |
| V2v | 7.8 | −71.1 | −3.3 | 4.0 | 5.9 | 5.9 | 100 |
| V2d | 8.2 | −87.6 | 6.1 | 3.5 | 4.3 | 4.5 | 100 |
| VP | 12.9 | −69.7 | −7.3 | 4.4 | 5.7 | 5.4 | 100 |
| V3 | 12.0 | −87.6 | 10.3 | 5.9 | 5.5 | 4.2 | 100 |
| V3a | 17.4 | −84.1 | 15.9 | 9.3 | 6.1 | 3.4 | 91 |
| V4 | 19.4 | −72.6 | −12.0 | 3.3 | 5.6 | 2.9 | 100 |
| V5 | 41.3 | −64.8 | −1.6 | 4.7 | 7.0 | 6.2 | 82 |
| Mean standard deviation | | | | 4.7 | 5.7 | 4.7 | |

significantly correlated with a correlation coefficient of 0.64 ($P < 0.0006$).

## Location variance

The mean functional-area variability in location across 17 areas tested was quite low (Table III, Fig. 4). The average standard deviation for all axes across all areas tested was 4.9 mm (95% confidence interval (CI), 4.5–5.4 mm). The mean standard deviation for the x-axis across all areas tested was 4.3 mm (95% CI, 3.4–5.2 mm), and for the y-axis, 5.3 mm (95% CI, 4.8–5.9 mm). The average standard deviation for the z-axis across all 17 areas tested was 5.2 mm (95% CI, 4.4–6.1 mm). When analyzed separately, the pooled standard deviation for all axes across all areas tested in the left hemisphere was 4.8 mm (95% CI, 4.2–5.5 mm). The pooled standard deviation for the x-axis across 9 areas tested in the left hemisphere was 3.9 mm (95% CI, 2.9–4.8 mm), and for the y-axis, 5.0 mm (95% CI, 4.2–5.9 mm). The average standard deviation for the z-axis across the 9 areas tested in the left hemisphere was 5.7 mm (95% CI, 4.3–7.0 mm).

Similarly, the pooled standard deviation for all axes across all 8 areas tested in the right hemisphere was 5.1 mm (95% CI, 3.8–6.3 mm). The mean standard deviations for x-, y-, and z-axes across the 8 areas tested in the right hemisphere were 4.7 mm (95% CI, 3.0–6.5 mm), 5.7 mm (95% CI, 5.1–6.4 mm), and 4.7 mm (95% CI, 3.7–5.7 mm), respectively .

## Difference between variances

In order to assess whether there was any difference in the ability of the Talairach space construct to reduce variability in one axis vs. another, we compared the mean standard deviations in the x-, y-, and z-axes in both hemispheres using a factorial ANOVA design. Our analysis indicated that side (hemisphere) had no significant effect ($P < 0.62$), but that the type of axis did have a subthreshold effect ($P < 0.08$). Therefore, we proceeded to further analyze the data using the paired t-test.

The difference between the mean standard deviations for the x- and y-axes (4.3 mm and 5.3 mm, respectively) averaged across all areas (both hemispheres) was statistically significant ($P < .05$). Within the left hemisphere, the mean standard deviation for the z-axis across the 9 areas tested (5.7 mm) was significantly greater ($P < 0.05$) than that for the x-axis

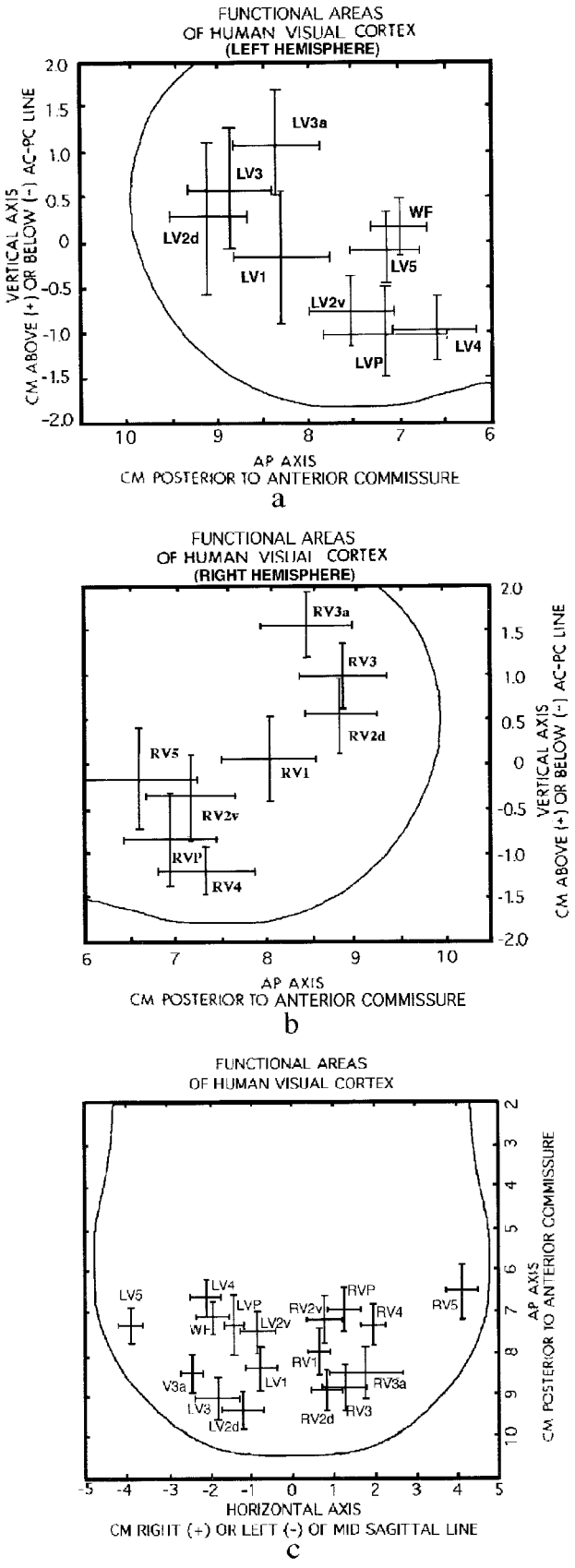


(3.9 mm). No statistically significant difference was found between the mean standard deviations for the x-, y-, and z-axes (4.7 mm, 5.7 mm, and 4.7 mm, respectively) in the right hemisphere. In addition, no statistically significant difference was found when the mean standard deviations for x-, y-, and z-axes in the left hemisphere were compared with their respective counterparts in the right hemisphere. Neither could any statistically significant difference be found between the pooled standard deviations across all axes in the left hemisphere (4.8 mm) vs. the pooled standard deviation across all axes in the right hemisphere (5.0 mm).

To further analyze whether normalization to Talairach space was equally effective in reducing variability within a particular axis across areas, the variances of different areas were examined for nonhomogeneity within each axis, using Bartlett's test. The location variances of functional areas of both hemispheres were surprisingly consistent for the y-axis ($P > 0.5$). The location variances for the z-axis were less consistent ($P > 0.35$ and $P > 0.08$ for right and left hemispheres, respectively). The only statistically significant difference between variances for a given axis was found in the x-axis of the right hemisphere between the variance of right V3a for the x-axis (0.86 $cm^2$) and the variances of right V1 and V4 for the x-axis(0.068 $cm^2$ and 0.11 $cm^2$, respectively).

Each of the individual areas was also analyzed for nonhomogeneity between variances in the three axes (Fig. 5) for that particular area. A total of 51 comparisons was made, three for each area ($s^2x$ vs. $s^2y$, $s^2x$ vs. $s^2z$, and $s^2y$ vs. $s^2z$). The variances for the x-axis of left V1, VP, V3a, and right V3a were found to be significantly different ($P < 0.05$) from their respective variances for the z-axis. The variances for the x-axis of right V1, V4, and left VP were significantly different from their respective variances for the y-axis ($P < 0.05$). Lastly, the variances for the y-axis of left V2d and right V4 were significantly different from their respective variances in the z-axis. Thus, out of 51 comparisons made, 9 were found to be statistically significant.

**Figure 4.**

Stereotactic plots of the human visual cortex. **a:** Mean locations in y- and z-axes for visual areas of the left hemisphere in 11 subjects, with bars representing one standard deviation. **b:** Mean locations in y- and z-axes for visual areas of the right hemisphere in 11 subjects, with bars representing one standard deviation. **c:** Mean locations in x- and y-axes for visual areas of both hemispheres in 11 subjects, with bars representing one standard deviation.

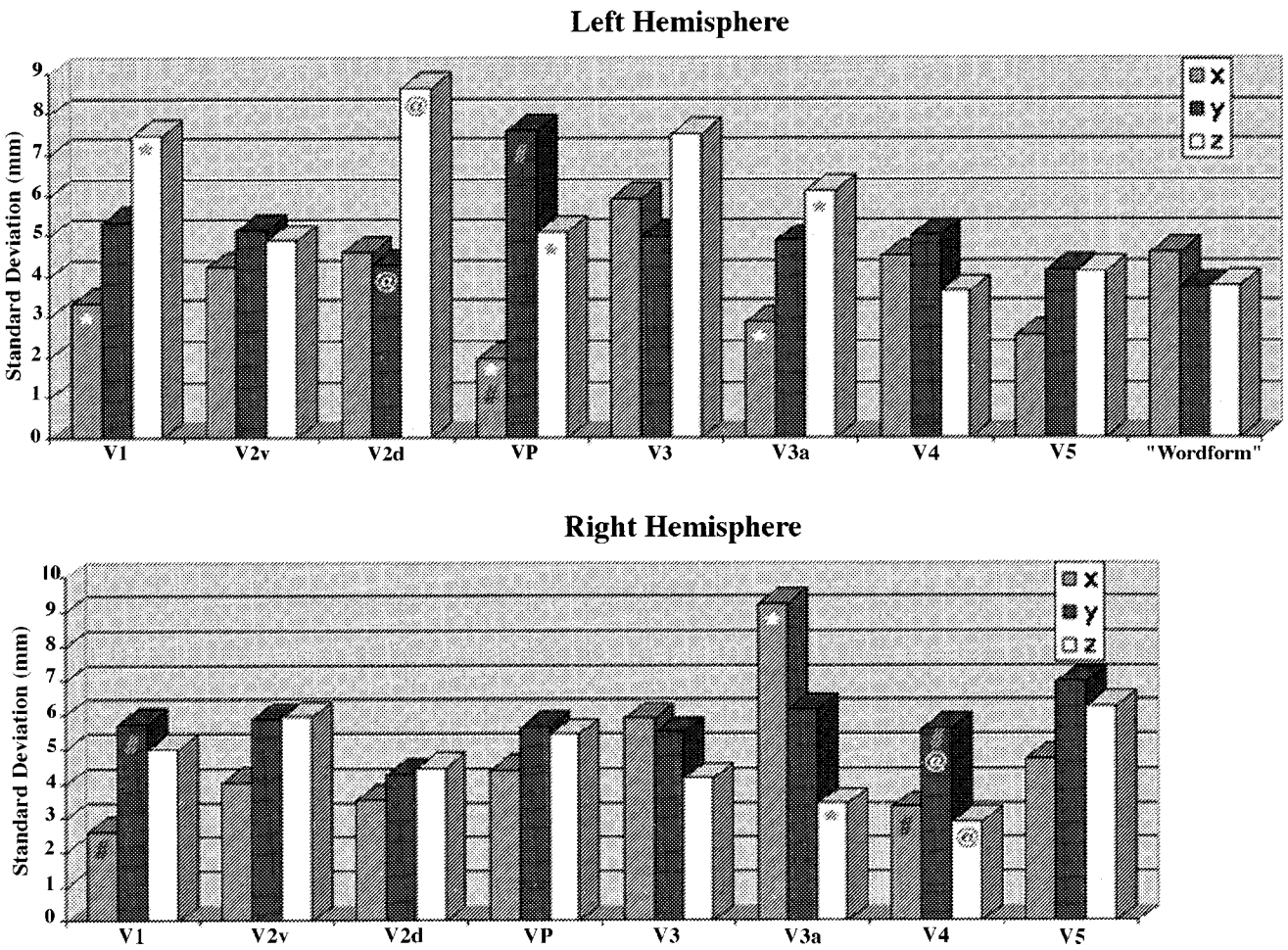


**Figure 5.**

Standard deviations for x-, y-, and z-axes of each area examined. *Significant ($P < 0.05$) difference between the variances for x- and z-axes. #Significant ($P < 0.05$) difference between the variances for x- and y-axes. @Significant ($P < 0.05$) difference between the variances for y- and z-axes.

### Normality of data

Since Bartlett's test for nonhomogeneity of variances assumes normal distribution of sampling points, we also analyzed the data for departures from normality. The Lillifor variant of the Kolmogrov-Smirnov test for goodness of fit was used because it is valid for sample sizes of 5 or greater. Out of 51 sets of coordinate data (17 for each axis) examined, none were found to be statistically different from a normal distribution ($P < 0.05$). However, x-axis coordinates for left V1 and left V5 showed a trend towards a departure from a normal distribution ($P < 0.09$ and $P < 0.06$, respectively). The rest of the data sets (49 out of 51; 96%) were found to have no significant difference from a normal distribution ($P > 0.2$). Since the tests for skew and kurtosis (gamma statistics) are applicable only for sample sizes $>20$, these tests were not employed (our sample size being 11 subjects).

The data sets for response magnitude were also tested for normality, and the response magnitudes for anterior border of right VP were the only data set found to be non-Gaussian ($P < 0.02$).

## DISCUSSION

There are at least three possible sources which could account for the observed variance in location. These include variability due to differences in brain size and shape (anatomic variability), potential difference in areas used for performing the same task (physiologic variability), and variability due to methodological considerations such as the particular scanner, the warping technique used, and the image reconstruction

algorithms. In our work we assume that at least for early visual processing such as form, color, and motion discrimination, the same areas are used across all individuals. Hence, we investigated anatomic variability remaining after normalization into Talairach space using a nine-parameter affine transform. It should be mentioned here that Hunton et al. [1996] found that using two PET cameras with different resolutions and sensitivities can lead to different estimates of variability. Thus, the mean standard deviation (SD) of x, y, and z locations using the PETT VI images (FWHM 17 mm) were 7.1 mm, 6.7 mm, and 6.2 mm, respectively. These were found to be significantly different from the mean SD of x, y, and z locations (5.1 mm, 5.2 mm, and 4.4 mm, respectively) when using an ECAT 935b camera with a resolution of 5.6 mm. In our study, the mean SD of x, y, and z locations was 4.3 mm, 5.3 mm, and 5.2 mm, respectively, using a GE/Scanditronix 4096 PET camera with a resolution of 6 mm.

Examination of anatomical location and its variability in proportional 3-D coordinates relative to the bicommissural plane is an important feature of this study. The strengths of reporting data in a well-defined mathematical construct are several. It allows for fully quantitative, parametric statistical manipulation and increased automation. It also makes brain mapping sufficiently reliable and rigorous for cross-study comparisons by providing a common frame of reference. It is interesting to note that we observed substantial activation at more advanced stages of visual processing (e.g., the "wordform" area) with a relatively simple stimulus. However, this area is known to participiate in the left lateralized object recognition system, assembling visual percepts and images [Parsons et al., 1995; Farah, 1991]. Our experiment strengthens the argument for a less strict specialization of this area. In addition, the inferior occipital area designated as human V4 by Zeki et al. [1991] also responded to our random dot stimulus. This could be due to two factors. The first is methodological, in that our projection system created white dots on a black background by superimposing isoluminant red, green, and blue dots with a minimal amount of chromatic aberration. However, this small amount of color dispersion is far from being the optimal stimulus for V4. More likely, V4 activation was probably due to a role that this area may play in addition to color processing. For example, the macaque area V4 plays a role in both hue and pattern discrimination [Heywood and Cowey, 1987]. Moreover, when this area is lesioned in monkeys, the predominant loss is in form discrimination [Heywood and Cowey, 1993]. In humans, Schneider et al. [1993] reported activations in the fusiform-lingual area (mean Talairach coordinates: 23, -11, and -74 for x-, y-, and z-axes, respectively) and in the posterior parietal lobe-superior occipital region to a black-and-white reversing checkerboard pattern. In accordance with this result, we found activation at these more advanced stages of processing with a relatively simple stimulus.

Another interesting observation was the lack of a strict correspondence between calcarine anatomy and the horizontal-meridian representation in 2 (both right hemispheres) out of 22 hemispheres. In one of these individuals the calcarine sulcus was between the contralateral horizontal- and the upper vertical-meridian (ventral V1/V2 border) representation, with the bulk of horizontal-meridian activation being on the cuneus immediately dorsal to the lip of the calcarine sulcus. Thus, even though the calcarine sulcus was within the confines of V1, the horizontal-meridian representation was not within the sulcus. In the other individual, the dorsal V1/V2 border representing the lower-visual-field vertical-meridian was found in the calcarine instead of the contralateral horizontal-meridian representation. These observations echo the original finding by Brodmann concerning area 17: "The borders of this area, especially laterally, are extraordinarily variable, which is particularly important for pathology. But even medially there are no regular and constant relationships to any limiting sulci ..." [Garey, 1994]. This finding has been confirmed by Rademacher et al. [1993], among others. The lack of a strict correspondence between sulcal and functional anatomy points to a clear need for an alternative to "gross space" for mapping the human brain. We support the use of a 3-D Cartesian construct such as the Talairach space for mapping and modeling the human brain.

As Figure 3 indicates, there is considerable variance in the borders and shape of a given visual area, even between the hemispheres of the same individual. The use of center of mass of an area simplifies this variance and provides a well-behaved location metric in a 3-D Cartesian construct. The mean standard deviation in location of the 17 visual areas tested was on the order of 5 mm in each of the x-, y-, and z-axes. The average standard deviation for the y-axis (5.3 mm) was statistically greater than that in the x-axis (4.3 mm) ($P < 0.05$). This may reflect a better ability of Talairach space to normalize in the x-axis than in the y-axis. However, the absolute difference between the two was only 1 mm. The mean standard deviation for the z-axis in the left hemisphere (5.7 mm) was statistically greater than that

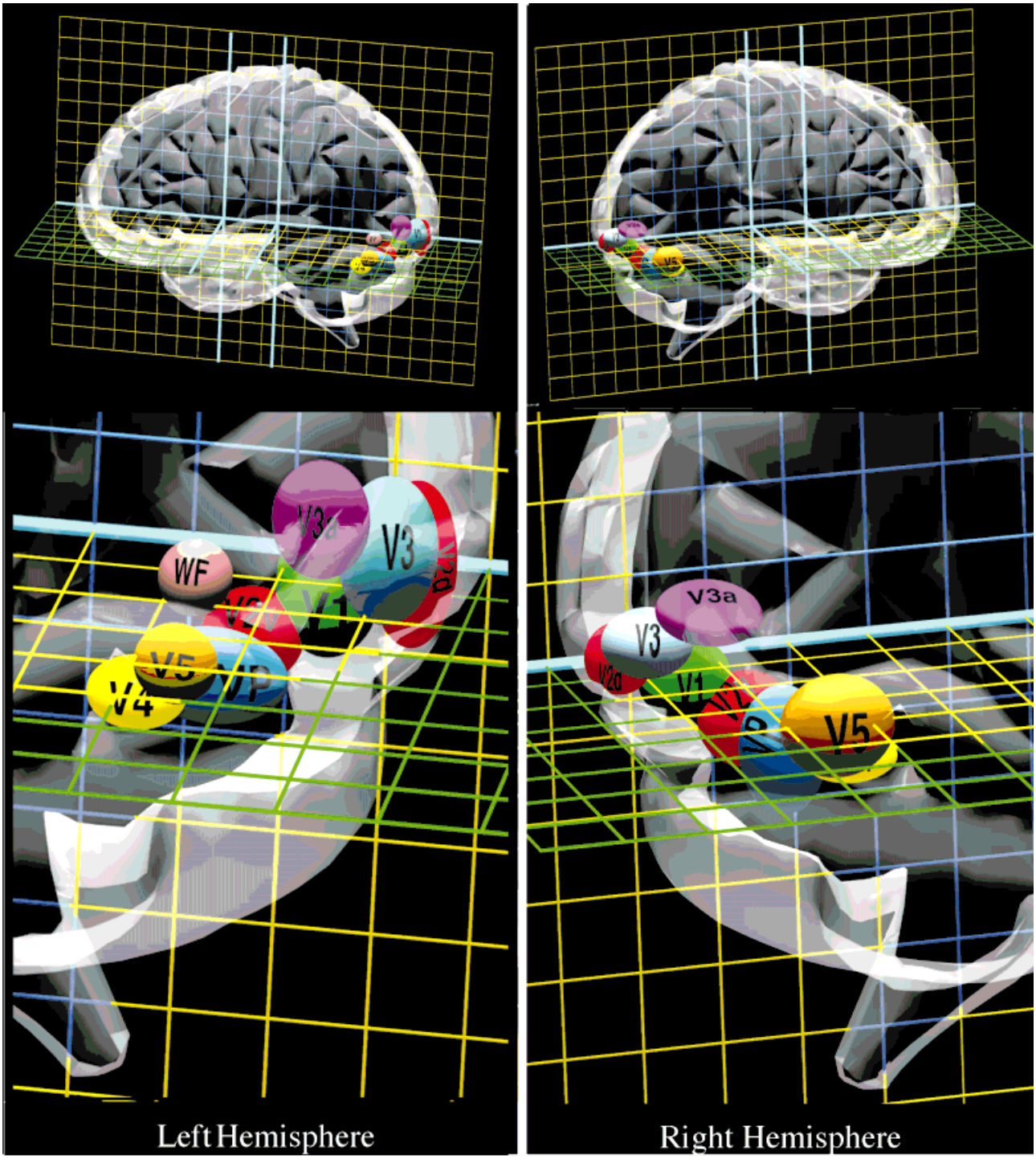


**Figure 6.**
Views of left and right hemispheres in Talairach space. Each square in the grid is 1 × 1 cm. The radius of each elipsoide is one standard deviation about its mean in each axis (the 3-D orientation here may not represent the actual 3-D distribution).

for the x-axis in the left hemisphere (3.9 mm). The occipital pole protrudes downwards on the left side in 77% of right-handed individuals, whereas it is wider on the left side in 66% of right-handed individuals [LeMay, 1977]. This gross anatomic variability may be reflected in the increased variance of functional area locations in the z-axis. Again, however, the absolute difference between the two standard deviations was <2 mm. Thus, as illustrated in Figure 6, the average residual anatomical variability after normalization into Talairach space was around 5 mm and essentially of the same magnitude in all axes.

Out of 51 comparisons made (3 for each area) for differences between location variability in x-, y-, and z-axes for a given functional area, 42 (82%) showed no statistically significant difference. Moreover, none of the variances for any area was >1 cm. This suggests that when studied in a 3-D Cartesian construct such as the Talairach space, the location variability for a particular area caused by the ontogenetic forces that shape the cerebral cortex is generally similar in all three axes.

The small average variability in location for areas in the occipital lobe implies that metanalysis can be applied to the locations of visual system operations in the human brain derived from different functional neuroimaging studies. This makes a strong argument for a functional volume modeling approach to cross-study analysis [Fox et al., 1997]. Most simply stated, the purpose of functional volume modeling is to extract spatial probability predictions that can be scaled for group size and which are derived from group mean studies of varying sample size and using varying imaging methods. A statistical assumption for functional volume modeling is that the underlying data have a Gaussian distribution. Our testing of the data for departures from normality revealed no statistically significant difference from normal distribution in any of the data. In 49 out of 51 data sets tested, this could be said with a high degree of confidence ($P >$ 0.2). The need for a probabilistic atlas becomes obvious when one compares the results obtained from an individual to a standard brain such as the one in the atlas of Talairach and Tournoux [1988]. In our comparison of V1 coordinates for each hemisphere with the V1 coordinates of this atlas, only 10 out of 22 hemispheres (45.5%) had the center-of-mass of V1 in the atlas Brodmann area 17, whereas one hemisphere's V1 coordinates were in the atlas cuneus. The rest of the 11 hemispheres had the center-of-mass of V1 in the atlas lingual gyrus.

The normality and statistically well-behaved nature of the data were confirmed when the coordinates for the right and the left V1 acquired from averaged data of the 11 subjects were compared with the mean coordinates for the right and the left V1 obtained from the same subjects individually (Table IV). The average difference between the two sets of coordinates was 1.3 mm, with the maximum difference being 2.3 mm.

**TABLE IV. Group averaged and group mean coordinates for V1**

| | Talairach coordinates | | |
|---|---|---|---|
| | Lx, Rx (mm) | Ly, Ry (mm) | Lz, Rz (mm) |
| Group averaged coordinates for V1 | −8.2, 5.0 | −81.0, −81.0 | 0.4, 1.7 |
| Mean coordinates of individual subjects for V1 | −7.2, 6.2 | −82.5, −79.9 | −1.9, 0.9 |

A possible weakness of this study concerning normality testing was the relatively small number of subjects. Even though the Lillifor variant of the Kolmogrov-Smirnov test for goodness of fit is applicable to sample sizes as low as 5, the statistical power of most tests for departures from normality increases with sample size. For example, parametric testing for skew and kurtosis (gamma statistics) could not be employed since these tests are valid only for sample sizes >20, whereas we had only 11 subjects. Moreover, the relatively small number of subjects prevented us from dividing the group into two subsets and analyzing intersubject replication.

A few other studies have reported on intersubject variability [Stensaas et al., 1974; Fox et al., 1987a,b; Grafton et al., 1991; Watson et al., 1993; Schneider et al., 1993; Rademacher et al., 1993; Ramsey et al., 1996; Hunton et al., 1996]. Of these studies, Fox et al. [1987a,b], Watson et al. [1993], Schneider et al. [1993], Ramsey et al. [1996], and Hunton et al. [1996] reported their results in a Cartesian stereotaxic reference space (thereby enabling generalization of results), finding intersubject standard deviations of 4–8 mm. Another paper from Fox and Pardo [1991] examined the standard deviations of responses to linguistic tasks in the occipital, cingulate, and frontal cortices and found standard deviations in the range of 3–10 mm. Thus, the findings of our study agree with these previous studies and extend the findings to multiple areas of the visual cortex.

Studies on cerebral plasticity, both as regards recovery after injury in patients and after training effects in normal volunteers, have important implications for

the cerebral organization of cognition and behavior. The mean locations and standard deviations for the visual areas reported in this study can provide reference values to test hypotheses concerning cerebral plasticity in the visual cortex.

## ACKNOWLEDGMENTS

We thank J. Roby, B. Heyl, and P. Jerabek for valuable technical assistance.

## REFERENCES

Clarke S, Miklossy J (1990): Occipital cortex in man: Organization of callosal connections, related myelo- and cytoarchitecture, and putative boundaries of functional visual areas. J Comp Neurol 298:188–214.

Daniel PM, Whitteridge D (1961): The representation of the visual field on the cerebral cortex in monkeys. J Physiol (Lond) 159:203–221.

DeYoe EA, Carman GJ, Bandettini P, Glickman S, Wieser J, Cox R, Miller D, Neitz J (1996): Mapping striate and extrastriate visual areas in human cerebral cortex. Proc Natl Acad Sci USA 93:2382–2386.

Farah MJ (1991): Visual Agnosia, Cambridge, MA: MIT Press.

Felleman DJ, Van Essen DC (1991): Distributed hierarchial processing in primate cerebral cortex. Cereb Cortex 1:1–47.

Fox PT, Pardo JV (1991): Does intersubject variability in cortical functional organization increase with neural ''distance'' from the periphery? Ciba Found Symp 163:125–144.

Fox PT, Raichle ME (1985): Stimulus rate determines regional blood flow in striate cortex demonstrated by positron emission tomography. Ann Neurol 17:303–305.

Fox PT, Fox JM, Raichle ME, Burde RM (1985): The role of cerebral cortex in the generation of voluntary saccades: A positron emission study. J Neurophysiol 54:348–369.

Fox PT, Mintun MA, Raichle ME, Miezin FM, Allman JM, Van Essen DC (1986): Mapping human visual cortex with positron emission tomography. Nature 323:806–809.

Fox PT, Miezen FM, Allman JM, Van Essen DC, Raichle ME (1987): Retinotopic organization of human visual cortex mapped with positron emission tomography. J Neurosci 7:913–922.

Fox PT, Burton H, Raichle ME (1987): Mapping human somatosensory cortex with positron emission tomography. J Neurosurg 67:34–43.

Fox PT, Mintun MA, Reiman EM, Raichle ME (1988): Enhanced detection of focal brain responses using intersubject averaging and change distribution analysis of subtracted PET images.

J Cereb Blood Flow Metab 8:642–653.

Fox PT, Lancaster JL, Parsons LM, Xiong J (1997): Functional volume modeling: Metanalytic models for statistical parametric imaging. Neuroimage 5:397.

Garey LJ (1994): Brodmann's ''Localization in the Cerebral Cortex.'' London: Smith-Gordan, pp 109–129.

Grafton ST, Woods RP, Mazziotta JC, Phelps ME (1991): Somatotopic mapping of the primary motor cortex in humans: Activation studies with cerebral blood flow and positron emmission tomography. J Neurophysiol 3:735–743.

Herscovitch P, Markham J, Raichle ME (1983): Brain blood flow measured with intravenous $H_2{}^{15}O$: I. Theory and error analysis. J Nucl Med 24:782–789.

Heywood CA, Cowey A (1987): On the role of cortical area V4 in the discrimination of hue and pattern in macaque monkeys. J Neurosci 7:2601–2617.

Heywood CA, Cowey A (1993): Colour and face perception in man and monkey: the missing link. In: Gulyas B, Ottoson D, Roland PE (eds): Functional Organization of the Human Visual Cortex. Wenner-Gren International Series, Volume 61. Pergamon Press, pp 195–210.

Holmes G (1945): The organization of the visual cortex in man. Proc R Soc Lond [Biol] 132:348–361.

Horton JC, Hoyt WF (1991): The representation of the visual field in human striate cortex. A revision of the classic Holmes map. Arch Ophthalmol 109:816–824.

Horton JC, Hoyt WF (1991): Quadrantic visual field defects; a hallmark of lesions in the extrastriate (V2/V3): Cortex. Brain 114:1703–1718.

Hunton DL, Miezin FM, Buckner RL, van Mier HI, Raichle ME, Petersen SE (1996): An assessment of functional-anatomical variability in neuroimaging studies. Hum Brain Mapp 4:122–139.

Lahti BP (1965): Signals, Systems and Communication. New York: Wiley, pp 437–441.

Lancaster JL, Glass TG, Lankipalli BR, Downs JH, Mayberg H, Fox PT (1995): A modality-independent approach to spatial normalization of tomographic images of the human brain. Human Brain Mapp 3:209–223.

LeMay M (1977): Asymmetries of the skull and handedness: Phrenology revisited. J Neurol Sci 32:243–253.

Parsons LM, Fox PT, Downs JH, Glass TG, Hirsch TB, Martin CC, Jerabek PA, Lancaster JL (1995): Use of implicit motor imagery for visual shape discrimination as revealed by PET. Nature 375:54–59.

Petersen SE, Fox PT, Snyder AZ, Raichle ME (1990): Activation of extrastriate and frontal cortical areas by visual words and word-like stimuli. Science 249:1041–1044.

Posner MI, Raichle ME (1994): Images of Mind. New York: Scientific American Library, pp 89–96.

Rademacher J, Caviness VS., Steinmetz H, Galaburda AM (1993): Topographical variation of the human primary cortices: Implications for neuroimaging, brain mapping, and neurobiology. Cereb Cortex 3:313–329.

Raichle ME (1987): Circulatory and metabolic correlates of brain function in normal humans. In: Handbook of Physiology—The Nervous System V. American Physiological Society, pp 643–674.

Raichle ME, Martin WRW, Herscovitch P, Mintun MA, Markham J (1983): Brain blood flow measured with intravenous $H_2{}^{15}O$. II. Implementation and validation. J Nucl Med 24:790–798.

Ramsey NF, Kirby BS, Gelderen PV, Berman KF, Duyn JH, Frank JA, Mattay VS, Van Horn JD, Esposito G, Moonen CTW, Weinberger DR (1996): Functional Mapping of human sensorimotor cortex with #D BOLD fMRI correlates highly with $H_2{}^{15}O$ PET rCBF. J Cereb Blood Flow Metab 16:755–764.

Schneider W, Casey BJ, Noll D (1993): Functional MRI mapping of stimulus rate effects across visual processing stages. Hum Brain Mapp 1:117–133.

Sereno MI, Dale AM, Reppas JB, Kwong KK, Belliveau JW, Brady TJ, Rosen BR, Tootell RBH (1995): Borders of multiple visual areas in

humans revealed by functional magnetic resonance imaging. Science 268:889–893.

Stensaas SS, Eddington DK, Dobelle WH (1974): The topography and variability of the primary visual cortex in man. J Neurosurg 40:747–755.

Talairach J, Tournoux P (1988): Principe et technique des études anatomiques. In: Rayport M (ed): Co-Planar Stereotaxic Atlas of the Human Brain—3-Dimensional Proportional System: An Approach to Cerebral Imaging, Volume 3. New York: Thieme Medical Publishers.

Watson JDG, Myers R, Frackowiak RSJ, Hajnal JV, Woods RP, Mazziotta JC, Shipp S, Zeki S (1993): Area V5 of the human brain. Cereb Cortex 3:79–94.

Woods RP, Mazziota JC, Cherry SR (1993): MRI-PET registration with automated algorithm. J Comput Assist Tomogr 17:536–546.

Zar JH (1984): Biostatistical Analysis, 2nd Edition . Englewood Cliffs, NJ: Prentice-Hall.

Zeki SM, Watson JD, Lueke CJ, Friston KJ, Kennard C, Frackowiak RSJ (1991): A direct demonstration of functional specialization in human visual cortex. J Neurosci 11:641–649.